

Modeling the Europa Plasma Torus

RON SCHREIER AND AHARON EVIATAR¹

Department of Geophysics and Planetary Sciences, The Raymond and Beverly Sackler Faculty of Exact Sciences, Tel Aviv University, Ramat Aviv, Israel

VYTENIS M. VASYLIŪNAS

Max-Planck-Institut für Aeronomie, Katlenburg-Lindau, Germany

JOHN D. RICHARDSON

Center for Space Research, Massachusetts Institute of Technology, Cambridge

The existence of a torus of plasma generated by sputtering from Jupiter's satellite Europa has long been suspected but never yet convincingly demonstrated. Temperature profiles from Voyager plasma observations indicate the presence of hot, possibly freshly picked-up ions in the general vicinity of the orbit of Europa, which may be interpreted as evidence for a local plasma torus. Studies of ion partitioning in the outer regions of the Io torus reveal that the oxygen to sulfur mixing ratio varies with radial distance; this may indicate that oxygen-rich matter is injected from a non-Io source, most probably Europa. We have constructed a quantitative model of a plasma torus near the orbit of Europa which takes into account plasma input from the Io torus, sputtering from the surface of Europa, a great number of ionization and charge exchange processes, and plasma loss by diffusive transport. When the transport time is chosen so that the model's total number density is consistent with the observed total plasma density, the contribution from Europa is found to be significant although not dominant. The model predicts in detail the ion composition, charge states, and the relative fractions of hot Europa-generated and (presumed) cold Io-generated ions. The results are generally consistent with observations from Voyager and can in principle (subject to limitations of data coverage) be confirmed in more detail by Ulysses.

INTRODUCTION

It has long been accepted that Io is the dominant source of plasma in the magnetosphere of Jupiter and that contributions from the icy satellites are insignificant. A reported detection of Europa-associated plasma in the Pioneer 10 data set [Intriligator and Miller, 1982] did not win broad acceptance. Early evaluations of the source strength of Europa ranged from $8 \times 10^{26} \text{ s}^{-1}$ from sputtering by radiation belt particles [Johnson *et al.*, 1981] down to as low as $3 \times 10^{24} \text{ s}^{-1}$ from sputtering by corotating iogenic ions [Eviatar *et al.*, 1981]. The latter estimate was made before the results of the low-energy sputtering experiments of Bar-Nun *et al.* [1985] became available and significantly undervalues the source rate. Later analyses by Sieveka and Johnson [1982] and Squyres *et al.* [1983] led to a deeper understanding of the interaction of the surface of Europa with the magnetosphere plasma [Eviatar *et al.*, 1985].

Bagenal [1989] reported a significant enhancement of a hot heavy-ion component outside the hot torus, as shown in Figure 1a, and suggested that this oxygen component might be associated with Europa.

These are preliminary results as the corrections for electron and ion feedthrough to the measured currents in the Plasma Science (PLS) instrument have not yet been fully

incorporated. Bagenal *et al.* [1992], in an investigation of the paucity of O^{++} in the Io torus reported by Brown *et al.* [1983], found that O^{++} pervades the entire magnetosphere and that while the sulfur density drops off with increasing radial distance, as expected, the oxygen does not. This again led to the suggestion that Europa may be playing a role as a magnetospheric plasma source. Renewed interest in the possibility of a Europa torus was stimulated by the Ulysses encounter with Jupiter. Observations made during the Ulysses flyby of Jupiter confirmed the existence of significant amounts of O^{++} in regions of the magnetosphere well off the geomagnetic equatorial plane [Geiss *et al.*, 1992]. The Ulysses instruments were turned off, however, during the close approach of the spacecraft to the planet, and no data were acquired in the equatorial plane. Our results complement the Ulysses ion mass spectrometer results as we strive to create a continuous latitudinal profile of plasma density and composition. This, of course, implies basic time independence, which is indeed a limitation of the validity of the conclusions. Confirmation of the Europa source hypothesis awaits more detailed analysis of the Ulysses plasma data set.

We present the results from a numerical model of the Europa torus. Sputtering from Europa's icy surface by magnetospheric particles is a source of molecular and atomic water fragments, and ionization and other atomic processes produce plasma in the vicinity of the satellite's orbit.

We first summarize what is known today about the plasma conditions near Europa. We then present the model and examine the effect of various parameters on the results, and compare the calculated density and composition with the

¹ Also at Department of Atmospheric Sciences, University of California, Los Angeles.

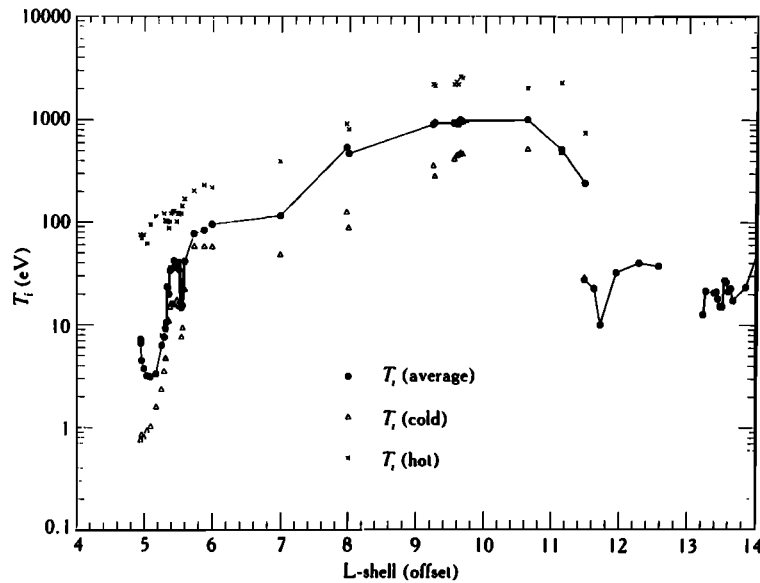


Fig. 1a. Radial profiles of the temperatures of various components of the ion plasma as observed by the PLS instrument on Voyager 1. The plot is taken from *Bagenal* [1989].

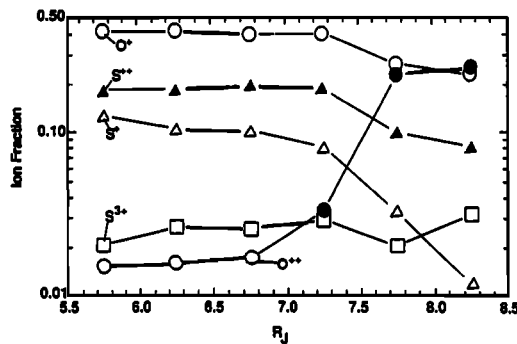


Fig. 1b. Ion partitioning from fits to UVS spectra (except O^{++} open circles which are from model calculations), taken from *Bagenal et al.* [1992].

observations. We also investigate the relative importance of iogenic and eurogenic sources in order to determine whether Europa provides a significant contribution to its plasma environment, that is, whether it is meaningful to discuss a Europa plasma torus.

EUROPA'S PLASMA ENVIRONMENT

The plasma conditions in the vicinity of Europa can be summarized as follows: The ion number density lies in the range 30 to 50 cm^{-3} [Belcher, 1983]. The temperature of the thermal or cold component rises from 50 – 60 eV at $L \sim 6$ to 200 – 400 eV at $L \sim 9$ – 11 , and there is an additional (30%) hot component at $\sim 2 \text{ keV}$ [Bagenal, 1989]. The hot component can be attributed to pickup ions created outside of Europa's orbit and heated adiabatically. The electron distribution function is also described by two components: a cold component (26 eV) with a number density of 36 cm^{-3} and a hot (1.2 keV) and tenuous component (3.1 cm^{-3}) of suprathermal electrons. Any successful model of a steady state torus must reproduce these observations of Europa's environment.

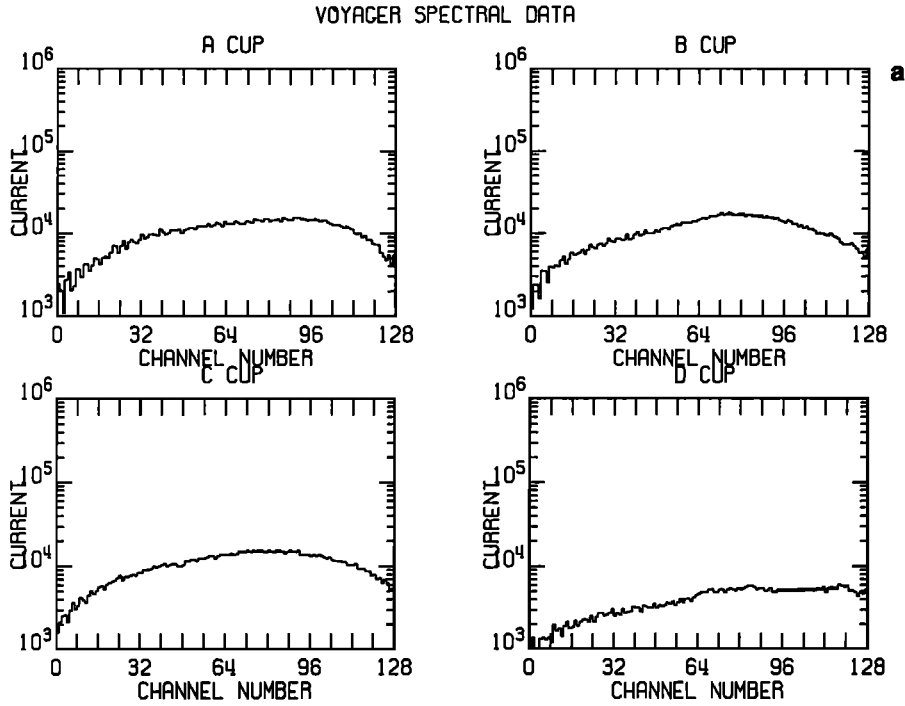
PLS OBSERVATIONS

The Voyager PLS instrument consists of four modulated-grid Faraday cups (A, B, C and D) which measure ions and electrons in the energy-per-charge range 10 to $5950 \text{ eV}/q$.

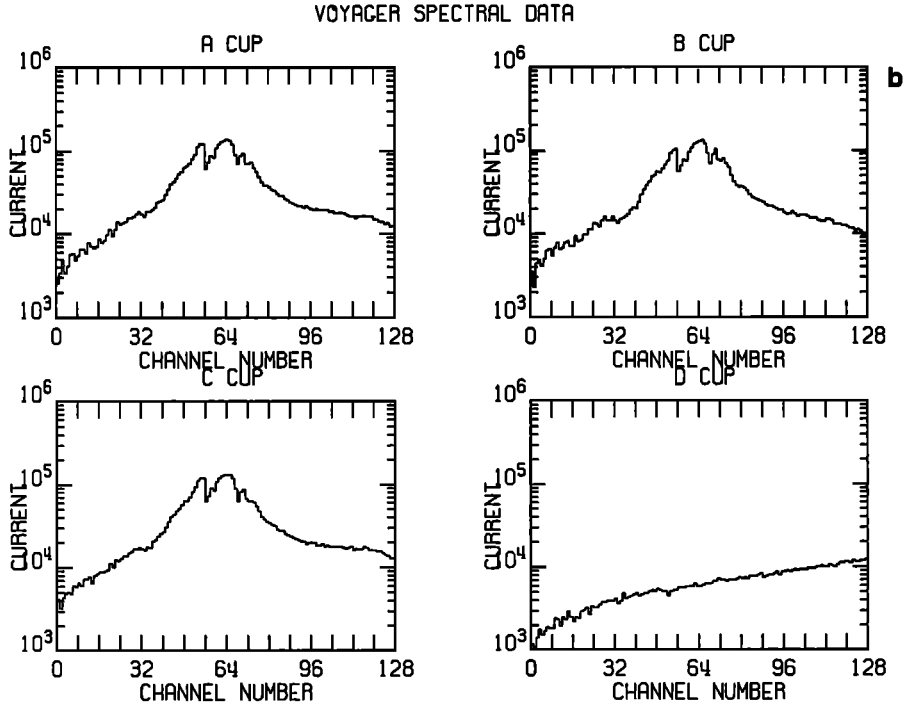
The main cluster consists of the A, B, and C cups, which are mounted about a cone whose central axis points toward Earth. The D cup points perpendicular to the spacecraft-Sun direction. When the spacecraft was inbound toward Jupiter, the D cup pointed approximately into the corotation direction during both the Voyager 1 and Voyager 2 encounters. A detailed description of the instrument and its modes of operation is given by *Bridge et al.* [1977]. This is an electrostatic instrument which has the capability to provide well-resolved particle spectra whenever the flow is cold and directed into the detectors. Such conditions held in the mid-magnetosphere plasma sheet [McNutt et al., 1981].

Figure 2 shows spectra from the Voyager 2 PLS instrument obtained near closest approach; the corresponding best fits (given the input assumptions) to these spectra are shown in the panels of Figure 3. The spectrum in Figure 2a is obtained $1.5 R_J$ south of the magnetic equator at a radial distance of $10.16 R_J$. Well-defined peaks appear in the A, B, and C cups. Figure 3a shows a fit to this spectrum using a Maxwellian plasma comprised of O^+ , S^+ , O^{++} , S^{3+} , Na^+ , and K^{++} [McNutt, this issue]. Another example of a spectrum in which well-defined peaks appear is shown in Figure 2b and its associated fit is shown by Figure 3b. Figure 2c presents a spectrum obtained at closest approach, outside the orbit of Europa at a similar distance ($1.5 R_J$) off the magnetic equator. Since the plasma is warm, the currents from individual species overlap. Nevertheless, this spectrum shows the presence of a hot locally picked-up background plasma as found by *Bagenal* [1989]. The crowding of six ion components into 50 energy channels (Figures 3a and 3b) prevents a unique determination of plasma parameters.

An agreement between a numerical model and the results obtained from the analysis of the PLS spectra is an important test for the model. Though the process of fitting ion distribution functions to the PLS spectra is not unique (i.e., the $A/Z=16$ component might be attributed either to O^+ and S^{++}), general characteristics of the model parameters (e.g., the total number density and the partitioning between (cold) iogenic and (hot) eurogenic plasma) should match those of the fits. The poor quality of the fits to the D cup currents may imply that significant electron feedthrough



JUPITER MAGNETOSPHERE
 $B = (-36.368, 44.816, -71.952)$ GAMMA
 VOYAGER 2 CHARGE DENSITY ESTIMATE = (11.9367)
 1979 190 2000:10.045 VCUP = $(96.509, 102.574, 103.225, 16.127)$ KM/S
 $R = 10.290$ $RHO(MAC) = 10.180$ $Z(MAC) = -1.506$ RIGID COROTATION SPEED = 127.763



JUPITER MAGNETOSPHERE
 $B = (-30.694, 48.933, -71.915)$ GAMMA
 VOYAGER 2 CHARGE DENSITY ESTIMATE = (41.8109)
 1979 190 2113:46.042 VCUP = $(100.068, 99.506, 98.880, 1.803)$ KM/S
 $R = 10.157$ $RHO(MAC) = 10.039$ $Z(MAC) = -1.549$ RIGID COROTATION SPEED = 125.995

Fig. 2. Plasma ion spectra obtained by Voyager 2 near closest approach of the spacecraft to the planet: (a) 1979 190 2013:46.042 UT, at radial distance of $10.157 R_J$, at centrifugal equator crossing; (b) 1979 190 2057:46.042 UT, at radial distance of $10.179 R_J$, at centrifugal equator crossing; (c) 1979 190 2000:10.045 UT; radial distance: $10.290 R_J$, $1.5 R_J$ below the equator.

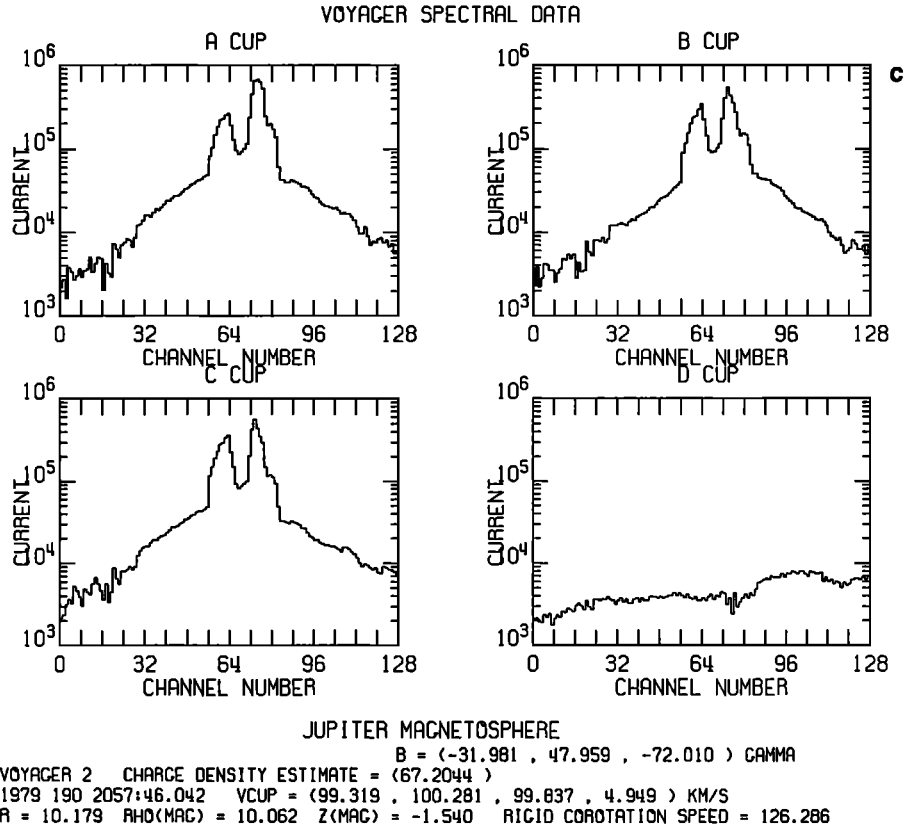


Fig. 2 (continued).

contamination occurs (Ralph L. McNutt, Jr., private communication, 1993). It is obvious that any material of European origin cannot be described simply by cold corotating Maxwellian distribution functions.

We shall discuss below the various possible interpretations of these findings, while bearing in mind that the hot temperature profile shown in Figure 1a is the signature expected from pickup of water group matter from Europa whereas the low temperature plasma observed near magnetic equator crossings is consistent with the idea of adiabatically cooled ion material.

MODELING THE TORUS

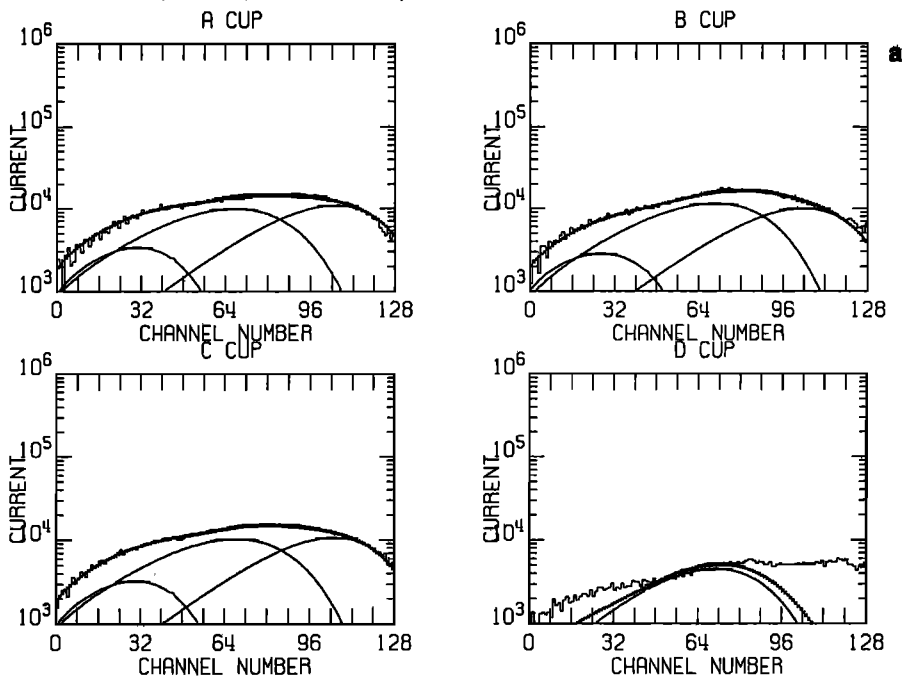
A planetary plasma torus is created by the effects of sunlight, corotating plasma and energetic particle fluxes [Eviatar *et al.*, 1978; Huang and Siscoe, 1987]. Its density, composition, and energy budget depend on the nature, composition, and strength of the source, radiative processes, atomic and molecular reactions, and the radial diffusion coefficient. If the source strength, transport rates, and reaction rates are given, we can determine the relative importance of iogenic and eurogenic matter.

In our model we include: (1) Sputtering of neutrals off the surface of Europa by sunlight, corotating ions, and energetic particles; (2) electron impact ionization and photoionization; (3) dissociative ionization of neutrals by photons and by electron impact; (4) charge exchange; (5) inflow by diffusion of iogenic plasma; and (6) loss of ions by diffusive flow and by collision with Europa. We use a "zero-dimensional" model similar to that which Richardson *et al.* [1986] used to describe the Kronian tori: iftwocol

$$\begin{aligned}
 \frac{dN_j^{(m,n)}}{dt} &= F_j^{(m,n)} \\
 &- \left[(\alpha_j + \beta_j)n_e + \eta_j^{(i)} + \eta_j^{(d)} \right. \\
 &\quad \left. + v \sum_k \sigma_{jk} n_k^{(a+m,i)} \right] N_j^{(m,n)} \\
 \frac{dN_j^{(m,i)}}{dt} &= \left[\alpha_j n_e + \eta_j^{(i)} + v \sum_{j \neq k} \sigma_{jk} n_k^{(a+m,i)} \right] N_j^{(m,n)} \\
 &- \left[\gamma_j^{(m)} n_e + v \sum_{k \neq j} \sigma_{kj} n_k^{(a+m,n)} + \frac{1}{\tau} + c \right] N_j^{(m,i)} \\
 \frac{dN_j^{(a,n)}}{dt} &= F_j^{(a,n)} \\
 &- \left[(\alpha_j + \beta_j)n_e + \eta_j^{(i)} + v \sum_k \sigma_{jk} n_k^{(a+m,i)} \right] N_j^{(a,m)} \\
 \frac{dN_j^{(a,i)}}{dt} &= I_j^{(a,i)} \\
 &+ \left[\alpha_j n_e + \eta_j^{(i)} + v \sum_{j \neq k} \sigma_{jk} n_k^{(a+m,i)} \right] N_j^{(a,n)} \\
 &- \left[\gamma_j^{(a)} n_e + v \sum_{k \neq j} \sigma_{kj} n_k^{(a+m,n)} + \frac{1}{\tau} + c \right] N_j^{(a,i)} \quad (1)
 \end{aligned}$$

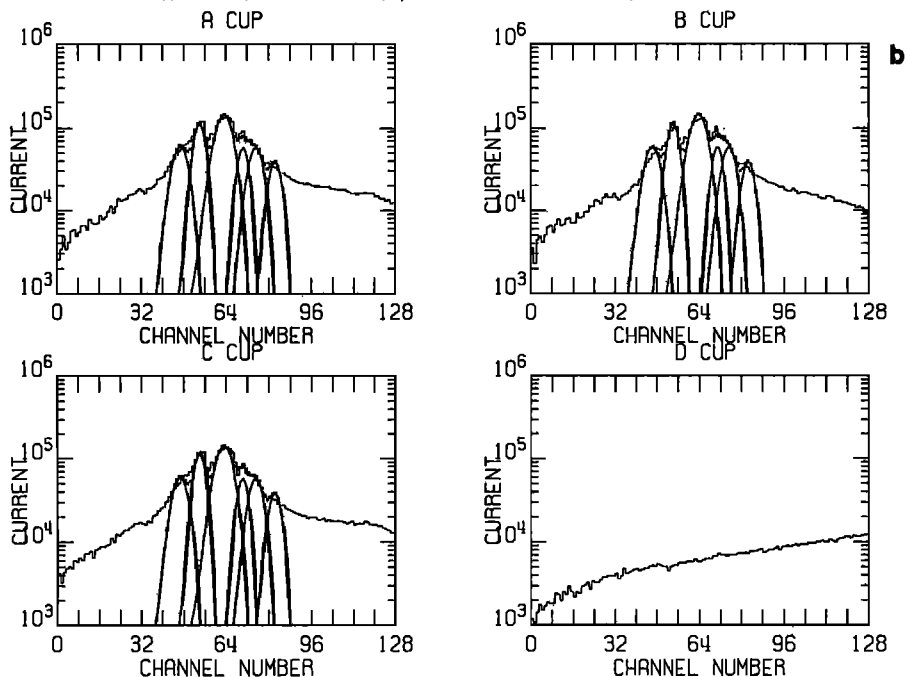
where the following notation has been used: The subscripts j and k denote individual species, the superscripts

ABSON: MAXWELLIAN SIMULATION , V2 AT JUPITER ON 1979 190 2000:10.045



V=(-19.107,127.883,-12.016) KM/S BCYL=(-36.368,44.816,-71.952) GAMMA ** BEST FIT **
 A,Z = 16,1 16,2 1,1
 N(CM-3) = 5.88 8.70 1.50
 WPER = 111.55 111.55 111.55
 WPAR = 111.55 111.55 111.55

ABSON: MAXWELLIAN SIMULATION , V2 AT JUPITER ON 1979 190 2113:46.042



V=(1.347,105.397,.365) KM/S BCYL=(-30.694,48.933,-71.915) GAMMA
 A,Z = 16,1 16,2 32,3 39,2 23,1 32,1
 N(CM-3) = 14.12 2.65 2.42 1.74 4.51 2.70
 WPER = 7.00 7.00 4.95 4.48 5.84 4.95
 WPAR = 7.00 7.00 4.95 4.48 5.84 4.95

Fig. 3. Best fit composition analysis for the spectrum shown in Figures 2a and 2b.

TABLE 1. Rates of Photoprocesses

Reaction	Rate, s ⁻¹	Reaction	Rate, s ⁻¹
H → H ⁺ + e ⁻	2.7E-9	H ₂ O → H ⁺ + OH + e ⁻	4.8E-10
H ₂ → H + H	1.26E-9	H ₂ O → O ⁺ + H ₂ + e ⁻	2.16E-10
H ₂ → H ⁺ + H + e ⁻	3.5E-10	H ₂ O → H ₂ O ⁺ + e ⁻	1.24E-8
H ₂ → H ₂ ⁺ + e ⁻	2.0E-9	O ₂ → O + O	2.2E-9
O → O ⁺ + e ⁻	7.84E-9	O ₂ → O ⁺ + O + e ⁻	1.87E-9
OH → O + H	1.85E-7	O ₂ → O ₂ ⁺ + e ⁻	1.9E-8
OH → OH ⁺ + e ⁻ *	1.2E-8	S → S ⁺ + e ⁻	4.07E-8
H ₂ O → H + OH	3.8E-7	SO → SO ⁺ + e ⁻	3.2E-8
H ₂ O → H ₂ + O	5.0E-8	SO ₂ → SO ₂ + e ⁻	4.07E-8
H ₂ O → H + H + O	2.2E-8	SO ₂ → S + O ₂	2.15E-6
H ₂ O → OH ⁺ + H + e ⁻	2.0E-9	SO ₂ → SO + O	7.0E-6

Data are from *Schmidt et al.* [1988]. Read 2.7E-9 as 2.7×10⁻⁹. Photoprocesses include ionization, dissociation and dissociative ionization of the nine neutral species included in the model.

* Ionization rate of OH was set equal to that of H₂O.

(m,n) , (m,i) , (a,n) , and (a,i) denote molecules, neutral and ionized and atoms, neutral and ionized, respectively. The superscripts $(a+m,i)$ and $(a+m,n)$ imply that k is to be summed over both atomic and molecular species. $F_j^{(m,n)}$ and $F_j^{(a,n)}$ denote the total output of neutral molecules and atoms from the satellite, $I_j^{(a,i)}$ is the input of ions of iogenic origin, α_j is the electron impact ionization rate coefficient, β_j the electron impact dissociation rate coefficient, $\eta_j^{(i)}$ the photoionization rate, $\eta_j^{(d)}$ the photodissociation rate, $\gamma^{(m)}$ and $\gamma^{(a)}$ the dissociative and dielectronic recombination rates, respectively, σ_{pq} the charge exchange cross section between neutral p and ion q , v the relative velocity between the reactants, $N_j^{(p,q)}$ the total population of constituent j which is of structure $s = m$ or a and charge state $c = n$ or i , $n_j(s,c) \equiv N_j(s,c)/V$ the density of constituent j , V the volume of the Europa torus, n_e is the electron density, τ is the transport loss time, and c is the collision frequency of ions with the satellite. For each constituent, F is given by

$$F = \pi a_E^2 [J_\nu + 4 \sum_k Y_{Ek} J_{Ek} + v_{CR} \sum_k Y_k n_k^{a+m,i}] \quad (2)$$

where $a_E = 1560$ km is the radius of Europa, $v_{CR} = 105$ km s⁻¹ the relative corotation speed at Europa orbit, J_ν the rate of photosputtering by sunlight (1.6×10^7 cm⁻² s⁻¹) for H and OH [Harrison and Schoen, 1967], J_E the flux density of energetic particles which sputter matter from the surface of Europa, taken as 6×10^8 cm⁻² s⁻¹ with 20% heavy ions [Sieveka and Johnson, 1982]. The summation represents the flux density of corotating ions and the Y values are the sputtering yields. Sputtering by energetic particles occurs over the entire surface of Europa because of their large gyroradii (hence the factor of 4), while the other factors affect only one side. In order to include transport from Io in the zero-dimensional equations (1), we parametrize the Io input rate and the diffusion transport by means of I_j and τ . The basis of this parametrization is given in the appendix. We use the Io torus ion partitioning at 8.25 R_J shown in Figure 1b (taken from *Bagenal et al.* [1992]) and a value of 5/3 for the ion average charge state (see results and discussion). Following *Bagenal et al.* [1992], the Io source is assumed to be composed of the ions O⁺, O⁺⁺, S⁺, S⁺⁺, S³⁺, Na⁺ and H⁺, in relative number percentage of 32.7, 41, 1.7, 13, 5, 3.3 and 3.3, respectively.

TABLE 2. Sputtering Yields Per Corotating Ion

Species	Heavy Ions	H ⁺
H ₂ O	9.5	0.6
O ₂	5.5	1.2
H ₂	6	0
H	11	0

Data are from *Bar-Nun et al.* [1985].

Matter sputtered off the surface of Europa will differ in composition and energy spectrum from Io torus matter. The heavy component will consist of water vapor and molecular oxygen. The escape fraction of the sputtered neutrals produced by cascade sputtering was estimated by *Sieveka and Johnson* [1982] as 0.83, and we multiplied the yield values by this factor. From the assumed energy partition of the escaping neutrals, one may estimate the half thickness of the neutral particle torus of Europa as approximately $\Delta r = 1 R_J$; the volume V of the torus is then $V = 2\pi r_E \times \pi(\Delta r)^2$, where r_E is the orbital radius of Europa.

Molecular ions of iogenic origin (e.g., SO₂⁺ or S₂⁺) found by *Bagenal* [1985] are unlikely to be found beyond the hot torus because dissociative recombination times for these ions are small compared to the transport time, and thus these ions are not included in our model. Iogenic alkali ions such as Na⁺ and K⁺⁺ [see *McNutt*, this issue] were included as sputterers but not in the atomic processes under consideration in the model, since as their abundance is low.

The various rate coefficients used in the model are listed in Tables 1 to 6.

The rate coefficients for the atomic and molecular processes can be calculated from Arrhenius' equation [*Bond et al.*, 1966]:

$$k = \alpha \times \left(\frac{T}{300}\right)^\beta \exp(-\gamma/T) \text{ cm}^3 \text{ s}^{-1}, \quad (3)$$

where T is the electron temperature at Europa's orbit in kelvin. Since the bi-Maxwellian electron distribution has a core component at 26 eV and a suprathermal halo at 1200 eV [*Sittler and Strobel*, 1987], Tables 3 and 4 list the α , β , and γ coefficients and the rate coefficient at both temperatures. For charge exchange (Table 5), a temperature of 1 keV was used in Arrhenius' equation for the ions.

In cases of an inconsistency among the published reaction values of the same process, we chose our value according to the following criteria: first priority was given to a graph

TABLE 3. Rates of Electron Impact Dissociation, Ionization, and Dissociative Ionization

Reaction	α	β	γ	$k(26 \text{ eV})$	$k(1.2 \text{ keV})$	Ref.
$\text{H} + e^- \rightarrow \text{H}^+ + 2e^-$				1.8E-8	2.8E-8	1
$\text{H}_2 + e^- \rightarrow \text{H} + \text{H} + e^-$	3.22E-9	0.35	102000	2.58E-8	1.4E-7	2
$\text{H}_2 + e^- \rightarrow \text{H}_2^+ + 2e^-$				2E-8	4E-8	3
$\text{H}_2 + e^- \rightarrow \text{H}^+ + \text{H} + 2e^-$				1.1E-7	6E-8	3
$\text{O} + e^- \rightarrow \text{O}^+ + 2e^-$				3.9E-8	8E-8	1
$\text{O}^+ + e^- \rightarrow \text{O}^{++} + 2e^-$				5E-9	3E-8	1
$\text{OH} + e^- \rightarrow \text{O} + \text{H} + e^-$				1E-8	2.02E-7	*
$\text{OH} + e^- \rightarrow \text{OH}^+ + 2e^-$				2E-8	7.2E-8	*
$\text{H}_2\text{O} + e^- \rightarrow \text{H}_2 + \text{O} + e^-$	9.43E-10	0.5	81234	2.28E-8	2.02E-7	4
$\text{H}_2\text{O} + e^- \rightarrow \text{OH} + \text{H} + e^-$	9.43E-10	0.5	59301	2.45E-8	2.02E-7	4
$\text{H}_2\text{O} + e^- \rightarrow \text{H}_2\text{O}^+ + 2e^-$				2E-8	7.2E-8	3
$\text{H}_2\text{O} + e^- \rightarrow \text{H}_2^+ + \text{O} + 2e^-$				6E-11	1.2E-9	3
$\text{H}_2\text{O} + e^- \rightarrow \text{O}^+ + \text{H}_2 + 2e^-$				6E-11	1.8E-9	3
$\text{H}_2\text{O} + e^- \rightarrow \text{OH}^+ + \text{H} + 2e^-$				3E-9	1.8E-8	3
$\text{H}_2\text{O} + e^- \rightarrow \text{H}^+ + \text{OH} + 2e^-$				1.2E-9	2E-8	3
$\text{O}_2 + e^- \rightarrow \text{O} + \text{O} + e^-$	9.43E-10	0.5	59417	2.45E-8	2.02E-7	4
$\text{O}_2 + e^- \rightarrow \text{O}_2^+ + 2e^-$				2E-8	1.6E-7	5
$\text{O}_2 + e^- \rightarrow \text{O}^+ + \text{O} + 2e^-$				2.4E-9	6E-8	5
$\text{S} + e^- \rightarrow \text{S}^+ + 2e^-$				1.6E-7	1E-7	6
$\text{S}^+ + e^- \rightarrow \text{S}^{++} + 2e^-$				2E-8	2E-8	6
$\text{S}^{++} + e^- \rightarrow \text{S}^{3+} + 2e^-$				7E-9	1E-8	6

Read 3.22E-9 as 3.22×10^{-9} . 1, Lotz [1967]; 2, Millar et al. [1990]; 3, Kieffer [1969]; 4, Schmidt et al. [1988]; 5, Banks and Kockarts [1973]; 6, Brown et al. [1982]. The α , β , and γ are coefficients of Arrhenius' equation. The calculated rates are given for both thermal and suprathermal electrons. Rates are in $\text{cm}^3 \text{s}^{-1}$.

* Ionization rate of OH was set equal to that of H_2O .

TABLE 4. Rates of Recombination

Reaction	α	β	γ	$k(26 \text{ eV})$	$k(1.2 \text{ keV})$
$\text{H}^+ + e^- \rightarrow \text{H}$	3.5E-12	-0.75	0	1.96E-14	1.1E-15
$\text{H}_2^+ + e^- \rightarrow \text{H} + \text{H}$	9.8E-9	-0.5	0	3.1E-10	4.55E-11
$\text{H}_2^+ + e^- \rightarrow \text{H}_2$	2.25E-7	-0.4	0	1.4E-8	3.06E-9
$\text{O}^+ + e^- \rightarrow \text{O} *$				4E-12	5E-14
$\text{O}^{++} + e^- \rightarrow \text{O}^+ *$				1.5E-11	1E-13
$\text{OH}^+ + e^- \rightarrow \text{O} + \text{H}$	7.5E-8	-0.5	0	2.37E-9	3.48E-10
$\text{H}_2\text{O}^+ + e^- \rightarrow \text{OH} + \text{H}$	2E-7	-0.5	0	6.31E-9	9.29E-10
$\text{H}_2\text{O}^+ + e^- \rightarrow \text{O} + \text{H}_2$	2E-7	-0.5	0	6.31E-9	9.29E-10
$\text{O}_2^+ + e^- \rightarrow \text{O} + \text{O}$	1.95E-7	-0.7	0	1.54E-9	1.06E-10
$\text{O}_2^+ + e^- \rightarrow \text{O}_2 \dagger$	4E-12		-0.7	0	3.17E-14
$\text{H}_3\text{O}^+ + e^- \rightarrow \text{H}_2\text{O} + \text{H}$	3.5E-7	-0.5	0	1.1E-8	1.63E-9
$\text{H}_3\text{O}^+ + e^- \rightarrow \text{OH} + \text{H}_2 \dagger$	2.34E-7	-0.5	0	7.4E-9	1.0E-9
$\text{H}_3\text{O}^+ + e^- \rightarrow \text{OH} + \text{H} + \text{H}$	6.5E-7	-0.5	0	2.05E-8	3.02E-9
$\text{H}_3^+ + e^- \rightarrow \text{H}_2 + \text{H}$	1.1E-11	-0.5	0	3.47E-13	5.11E-14
$\text{H}_3^+ + e^- \rightarrow \text{H} + \text{H} + \text{H}$	1.1E-11	-0.5	0	3.47E-13	5.11E-14
$\text{O}_2\text{H}^+ + e^- \rightarrow \text{O}_2 + \text{H}$	3E-7	-0.5	0	9.47E-9	1.39E-9
$\text{S}^+ + e^- \rightarrow \text{S} *$				7E-12	5E-14
$\text{S}^{++} + e^- \rightarrow \text{S}^+ *$				3E-11	1E-13
$\text{S}^{3+} + e^- \rightarrow \text{S}^{++} *$				1E-10	2E-13
$\text{SO}^+ + e^- \rightarrow \text{S} + \text{O}$	2E-7	-0.5	0	6.31E-9	9.29E-10
$\text{S}_2^+ + e^- \rightarrow \text{S} + \text{S}$	2E-7	-0.5	0	6.31E-9	9.29E-10
$\text{SO}_2^+ + e^- \rightarrow \text{SO} + \text{S}$	1E-7	-0.5	0	3.1E-9	4.64E-10
$\text{HS}^+ + e^- \rightarrow \text{S} + \text{H}$	2E-7	-0.5	0	6.31E-9	9.29E-10
$\text{H}_2\text{S}^+ + e^- \rightarrow \text{S} + \text{H} + \text{H}$	1.5E-7	-0.5	0	4.37E-9	6.97E-10
$\text{H}_2\text{S}^+ + e^- \rightarrow \text{HS} + \text{H}$	1.5E-7	-0.5	0	4.37E-9	6.97E-10
$\text{HSO}^+ + e^- \rightarrow \text{SO} + \text{H}$	2E-7	-0.5	0	6.31E-9	9.29E-10
$\text{S}_2\text{H}^+ + e^- \rightarrow \text{S}_2 + \text{H}$	1.5E-7	-0.5	0	4.37E-9	6.97E-10
$\text{S}_2\text{H}^+ + e^- \rightarrow \text{HS} + \text{S}$	1.5E-7	-0.5	0	4.37E-9	6.97E-10
$\text{HSO}_2^+ + e^- \rightarrow \text{SO}_2 + \text{H}$	2E-7	-0.5	0	6.31E-9	9.29E-10
$\text{HSO}_2^+ + e^- \rightarrow \text{SO} + \text{H} + \text{O}$	1E-7	-0.5	0	3.1E-9	4.64E-10
$\text{HSO}_2^+ + e^- \rightarrow \text{SO} + \text{OH}$	1E-7	-0.5	0	3.1E-9	4.64E-10

Data are from Millar et al. [1991]. Read 3.5E-12 as 3.5×10^{-12} . Rates are in $\text{cm}^3 \text{s}^{-1}$.

* Brown et al. [1982].

† Schmidt et al. [1988].

TABLE 5. Rates of Charge Exchange

Reaction	α	β	γ	$k(1 \text{ keV})$
$\text{H}^+ + \text{H} \rightarrow \text{H}_2^+$	$2E-20$	1	0	$7.7E-16$
$\text{H}^+ + \text{H} \rightarrow \text{H} + \text{H}^+ *$				$3.5E-8$
$\text{H}^+ + \text{O} \rightarrow \text{H} + \text{O}^+$	$7E-10$	0	232	$7E-10$
$\text{H}^+ + \text{OH} \rightarrow \text{OH}^+ + \text{H}$	$2.1E-9$	0	0	$2.1E-9$
$\text{H}^+ + \text{H}_2 \rightarrow \text{H} + \text{H}_2^+$	$1E-10$	0	21200	$1E-10$
$\text{H}^+ + \text{H}_2\text{O} \rightarrow \text{H} + \text{H}_2\text{O}^+$	$8.2E-9$	0	0	$8.2E-9$
$\text{H}^+ + \text{O}_2 \rightarrow \text{H} + \text{O}_2^+$	$1.17E-9$	0	0	$1.17E-9$
$\text{H}^+ + \text{S} \rightarrow \text{S}^+ + \text{H}$	$1.3E-9$	0	0	$1.3E-9$
$\text{H}^+ + \text{SO} \rightarrow \text{SO}^+ + \text{H}$	$3.2E-9$	0	0	$3.2E-9$
$\text{H}^+ + \text{S}_2 \rightarrow \text{S}_2^+ + \text{H}$	$3E-9$	0	0	$3E-9$
$\text{H}_2^+ + \text{H} \rightarrow \text{H}_2 + \text{H}^+$	$6.4E-10$	0	0	$6.4E-10$
$\text{H}_2^+ + \text{H}_2 \rightarrow \text{H}_3^+ + \text{H}$	$2.08E-9$	0	0	$2.08E-9$
$\text{H}_2^+ + \text{H}_2 \rightarrow \text{H}_2 + \text{H}_2^+ \dagger$	$3.6E-9$	0	0	$3.6E-9$
$\text{H}_2^+ + \text{O} \rightarrow \text{OH}^+ + \text{H}$	$1E-9$	0	0	$1E-9$
$\text{H}_2^+ + \text{OH} \rightarrow \text{OH}^+ + \text{H}_2$	$7.6E-10$	0	0	$7.6E-10$
$\text{H}_2^+ + \text{OH} \rightarrow \text{H}_2\text{O}^+ + \text{H}$	$7.6E-10$	0	0	$7.6E-10$
$\text{H}_2^+ + \text{H}_2\text{O} \rightarrow \text{H}_3\text{O}^+ + \text{H}$	$3.4E-9$	0	0	$3.4E-9$
$\text{H}_2^+ + \text{H}_2\text{O} \rightarrow \text{H}_2\text{O}^+ + \text{H}_2$	$3.9E-9$	0	0	$3.9E-9$
$\text{H}_2^+ + \text{O}_2 \rightarrow \text{H} + \text{O}_2\text{H}^+$	$1.9E-9$	0	0	$1.9E-9$
$\text{H}_2^+ + \text{O}_2 \rightarrow \text{H}_2 + \text{O}_2^+$	$8E-10$	0	0	$8E-10$
$\text{H}_3^+ + \text{H}_2\text{O} \rightarrow \text{H}_3\text{O}^+ + \text{H}_2$	$5.9E-9$	0	0	$5.9E-9$
$\text{H}_3^+ + \text{O} \rightarrow \text{OH}^+ + \text{H}_2$	$8E-10$	0	0	$8E-10$
$\text{H}_3^+ + \text{OH} \rightarrow \text{H}_2\text{O}^+ + \text{H}_2$	$1.3E-9$	0	0	$1.3E-9$
$\text{H}_3^+ + \text{O}_2 \rightarrow \text{O}_2\text{H}^+ + \text{H}_2$	$5E-9$	0	150	$5E-9$
$\text{H}_3^+ + \text{S} \rightarrow \text{HS}^+ + \text{H}_2$	$2.6E-9$	0	0	$2.6E-9$
$\text{H}_3^+ + \text{SO} \rightarrow \text{HSO}^+ + \text{H}_2$	$1.9E-9$	0	0	$1.9E-9$
$\text{H}_3^+ + \text{S}_2 \rightarrow \text{S}_2\text{H}^+ + \text{H}_2$	$2.0E-9$	0	0	$2.0E-9$
$\text{H}_3^+ + \text{SO}_2 \rightarrow \text{HSO}_2^+ + \text{H}_2$	$1.3E-9$	0	0	$1.3E-9$
$\text{O}^+ + \text{H} \rightarrow \text{H}^+ + \text{O}$	$6.8E-10$	0	0	$6.8E-10$
$\text{O}^+ + \text{H}_2 \rightarrow \text{OH}^+ + \text{H}$	$1.7E-9$	0	0	$1.7E-9$
$\text{O}^+ + \text{O} \rightarrow \text{O} + \text{O}^+ \ddagger$				$1.8E-8$
$\text{O}^+ + \text{OH} \rightarrow \text{OH}^+ + \text{O}$	$3.6E-10$	0	0	$3.6E-10$
$\text{O}^+ + \text{OH} \rightarrow \text{H}^+ + \text{O}_2$	$3.6E-10$	0	0	$3.6E-10$
$\text{O}^+ + \text{H}_2\text{O} \rightarrow \text{H}_2\text{O}^+ + \text{O}$	$3.2E-10$	0	0	$3.2E-10$
$\text{O}^+ + \text{O}_2 \rightarrow \text{O}_2^+ + \text{O}$	$1.9E-11$	0	0	$1.9E-11$
$\text{O}^+ + \text{SO}_2 \rightarrow \text{O}_2^+ + \text{SO}$	$8E-10$	0	0	$8E-10$
$\text{OH}^+ + \text{H}_2 \rightarrow \text{H}_2\text{O}^+ + \text{H}$	$1.01E-9$	0	0	$1.01E-9$
$\text{OH}^+ + \text{OH} \rightarrow \text{H}_2\text{O}^+ + \text{O}$	$7E-10$	0	0	$7E-10$
$\text{OH}^+ + \text{O} \rightarrow \text{O}_2^+ + \text{H}$	$7.1E-10$	0	0	$7.1E-10$
$\text{OH}^+ + \text{H}_2\text{O} \rightarrow \text{H}_3\text{O}^+ + \text{O}$	$1.3E-9$	0	0	$1.3E-9$
$\text{OH}^+ + \text{H}_2\text{O} \rightarrow \text{H}_2\text{O}^+ + \text{OH}$	$1.59E-9$	0	0	$1.59E-9$
$\text{OH}^+ + \text{O}_2 \rightarrow \text{O}_2^+ + \text{OH}$	$5.9E-10$	0	0	$5.9E-10$
$\text{OH}^+ + \text{S} \rightarrow \text{S}^+ + \text{OH}$	$4.3E-10$	0	0	$4.3E-10$
$\text{OH}^+ + \text{S} \rightarrow \text{SO}^+ + \text{H}$	$4.3E-10$	0	0	$4.3E-10$
$\text{OH}^+ + \text{S} \rightarrow \text{HS}^+ + \text{O}$	$4.3E-10$	0	0	$4.3E-10$
$\text{H}_2\text{O}^+ + \text{H}_2 \rightarrow \text{H}_3\text{O}^+ + \text{H}$	$8.3E-10$	0	0	$8.3E-10$
$\text{H}_2\text{O}^+ + \text{O} \rightarrow \text{O}_2^+ + \text{H}_2$	$4E-11$	0	0	$4E-11$
$\text{H}_2\text{O}^+ + \text{OH} \rightarrow \text{H}_3\text{O}^+ + \text{O}$	$6.9E-10$	0	0	$6.9E-10$
$\text{H}_2\text{O}^+ + \text{H}_2\text{O} \rightarrow \text{H}_3\text{O}^+ + \text{OH}$	$2.1E-9$	0	0	$2.1E-9$
$\text{H}_2\text{O}^+ + \text{O}_2 \rightarrow \text{O}_2^+ + \text{H}_2\text{O}$	$4.3E-10$	0	0	$4.3E-10$
$\text{H}_2\text{O}^+ + \text{S} \rightarrow \text{S}^+ + \text{H}_2\text{O}$	$4.3E-10$	0	0	$4.3E-10$
$\text{H}_2\text{O}^+ + \text{S} \rightarrow \text{HSO}^+ + \text{H}$	$4.3E-10$	0	0	$4.3E-10$
$\text{H}_2\text{O}^+ + \text{S} \rightarrow \text{HS}^+ + \text{OH}$	$4.3E-10$	0	0	$4.3E-10$
$\text{H}_3\text{O}^+ + \text{S}_2 \rightarrow \text{S}_2\text{H}^+ + \text{H}_2\text{O}$	$2.0E-9$	0	0	$2.0E-9$
$\text{O}_2^+ + \text{O}_2 \rightarrow \text{O}_2 + \text{O}_2^+ \S$				$1.3E-8$
$\text{O}_2^+ + \text{H}_2 \rightarrow \text{O}_2\text{H}^+ + \text{H} \parallel$				$2.5E-9$
$\text{O}_2^+ + \text{S} \rightarrow \text{S}^+ + \text{O}_2$	$5.4E-10$	0	0	$5.4E-10$
$\text{O}_2^+ + \text{S} \rightarrow \text{SO}^+ + \text{O}$	$5.4E-10$	0	0	$5.4E-10$
$\text{O}_2\text{H}^+ + \text{O} \rightarrow \text{OH} + \text{O}_2$	$6.2E-10$	0	0	$6.2E-10$
$\text{O}_2\text{H}^+ + \text{S} \rightarrow \text{HS}^+ + \text{O}_2$	$1.1E-9$	0	0	$1.1E-9$
$\text{O}_2\text{H}^+ + \text{H}_2 \rightarrow \text{H}_3^+ + \text{O}_2$	$6.4E-10$	0	0	$6.4E-10$
$\text{O}_2\text{H}^+ + \text{OH} \rightarrow \text{H}_2\text{O}^+ + \text{O}_2$	$6.1E-10$	0	0	$6.1E-10$
$\text{O}_2\text{H}^+ + \text{H}_2\text{O} \rightarrow \text{H}_3\text{O}^+ + \text{O}_2$	$8.2E-10$	0	0	$8.2E-10$
$\text{S}^+ + \text{O}_2 \rightarrow \text{O}^+ + \text{SO} \P$	$2E-11$	0	0	$2E-11$
$\text{S}^+ + \text{O}_2 \rightarrow \text{SO}^+ + \text{O}$	$1.5E-11$	0	0	$1.5E-11$
$\text{S}^+ + \text{H}_2 \rightarrow \text{HS}^+ + \text{H}$	$1.1E-10$	0	9860	$1.1E-10$
$\text{S}^+ + \text{H}_2 \rightarrow \text{H}_2\text{S}^+$	$1E-17$	0	0	$1E-17$
$\text{S}^+ + \text{OH} \rightarrow \text{SO}^+ + \text{H}$	$6.1E-10$	0	0	$6.1E-10$
$\text{SO}_2^+ + \text{H}_2 \rightarrow \text{HSO}_2^+ + \text{H}$	$1.7E-11$	0	0	$1.7E-11$
$\text{SO}_2^+ + \text{O}_2 \rightarrow \text{O}_2^+ + \text{SO}_2$	$2.5E-10$	0	0	$2.5E-10$
$\text{HS}^+ + \text{H} \rightarrow \text{S}^+ + \text{H}_2$	$1.1E-10$	0	0	$1.1E-10$

TABLE 5. (continued)

Reaction	α	β	γ	$k(1 \text{ keV})$
$\text{HS}^+ + \text{H}_2 \rightarrow \text{H}_2\text{S}^+ + \text{H}$	$2E-10$	0	6380	$2E-10$
$\text{HS}^+ + \text{H}_2 \rightarrow \text{H}_3\text{S}^+$	$2.4E-16$	-0.8	0	$3.2E-19$
$\text{HS}^+ + \text{O} \rightarrow \text{SO}^+ + \text{H}$	$2.9E-10$	0	0	$2.9E-10$
$\text{HS}^+ + \text{O} \rightarrow \text{S}^+ + \text{OH}$	$2.9E-10$	0	0	$2.9E-10$
$\text{HS}^+ + \text{H}_2\text{O} \rightarrow \text{H}_3\text{O}^+ + \text{S}$	$7.8E-10$	0	0	$7.8E-10$
$\text{HS}^+ + \text{S} \rightarrow \text{S}^+ + \text{HS}$	$9.7E-10$	0	0	$9.7E-10$
$\text{H}_2\text{S}^+ + \text{H} \rightarrow \text{HS}^+ + \text{H}_2$	$2E-10$	0	0	$2E-10$
$\text{H}_2\text{S}^+ + \text{H}_2 \rightarrow \text{H}_3\text{S}^+ + \text{H}$	$6E-10$	0	2900	$6E-10$
$\text{H}_2\text{S}^+ + \text{O} \rightarrow \text{HS}^+ + \text{OH}$	$3.1E-10$	0	0	$3.1E-10$
$\text{H}_2\text{S}^+ + \text{O} \rightarrow \text{SO}^+ + \text{H}_2$	$3.1E-10$	0	0	$3.1E-10$
$\text{H}_2\text{S}^+ + \text{H}_2\text{O} \rightarrow \text{H}_3\text{O}^+ + \text{HS}$	$8.1E-10$	0	0	$8.1E-10$
$\text{H}_3\text{S}^+ + \text{H} \rightarrow \text{H}_2\text{S}^+ + \text{H}_2$	$6E-11$	0	0	$6E-11$
$\text{S}_2\text{H}^+ + \text{H}_2\text{S} \rightarrow \text{H}_3\text{S}^+ + \text{S}_2$	$2.9E-10$	0	0	$2.9E-10$
$\text{HSO}_2^+ + \text{H}_2\text{O} \rightarrow \text{H}_3\text{O}^+ + \text{SO}_2$	$2.13E-9$	0	0	$2.13E-9$

Data are from Millar et al. [1991]. Read $2E-20$ as 2×10^{-20} . Rates are in $\text{cm}^3 \text{s}^{-1}$.

* Newman et al. [1982].

† Massey and Gilbody [1974].

‡ Stebbings et al. [1964].

§ Banks and Kockarts [1973].

¶ Fehsenfeld et al. [1967].

|| Schmidt et al. [1988].

TABLE 6. Steady State Densities of the Torus Model

	Case a	Case b	Case c	Case d	Case e
$D_E, R_J^2 \text{ s}^{-1}$	4×10^{-4}	4×10^{-4}	4×10^{-4}	4×10^{-4}	2×10^{-4}
Io's source strength, amu/s	6×10^{29}	6×10^{29}	3×10^{29}	1.2×10^{30}	6×10^{29}
Energetic particles flux, $\text{cm}^{-2} \text{ s}^{-1}$	6×10^8	1.2×10^9	6×10^8	6×10^8	6×10^8
Neutral Species					
H	13.6 (0)	20 (0)	20 (0)	10 (0)	9.6 (0)
H ₂	0.4 (0)	0.6 (0)	0.5 (0)	0.3 (0)	0.3 (0)
O	5 (0)	7.4 (0)	7 (0)	3.5 (0)	3.3 (0)
O ₂	1.5 (0)	2.4 (0)	2 (0)	1 (0)	1 (0)
OH	1.3 (0)	2 (0)	1.6 (0)	1 (0)	0.9 (0)
H ₂ O	1.3 (0)	2 (0)	1.6 (0)	1 (0)	1 (0)
Major Ion Species					
H ⁺	3.5 (1.3)	4.7 (1.3)	2.4 (0.7)	5.8 (2.6)	9 (2.6)
O ⁺	15 (12.6)	16 (12.6)	8.3 (6.4)	27 (24)	28 (23)
O ⁺⁺	17.1 (16.9)	17.1 (16.9)	8.4 (8.4)	34.9 (34.7)	37.5 (36.3)
O ₂ ⁺	0.3 (0)	0.5 (0)	0.2 (0)	0.4 (0)	0.8 (0)
OH ⁺	0.2 (0)	0.4 (0)	0.2 (0)	0.4 (0)	0.7 (0)
H ₂ O ⁺	0.2 (0)	0.3 (0)	0.2 (0)	0.3 (0)	0.5 (0)
S ⁺	0.6 (0.6)	0.6 (0.6)	0.3 (0.3)	1 (1)	0.8 (0.9)
S ⁺⁺	5 (5)	5 (5)	2.5 (2.6)	9.7 (9.8)	9 (9)
S ³⁺	2.3 (2.3)	2.3 (2.3)	1 (1)	5 (5)	6 (6)
Na ⁺	1.3 (1.3)	1.3 (1.3)	0.7 (0.7)	2.6 (2.6)	2.6 (2.6)
Minor Ion Species					
H ₂ ⁺	0.06 (0)	0.09 (0)	0.05 (0)	0.07 (0)	0.13 (0)
H ₃ ⁺	$5 \cdot 10^{-6}$ (0)	$1 \cdot 10^{-5}$ (0)	$5 \cdot 10^{-6}$ (0)	$4 \cdot 10^{-6}$ (0)	$2 \cdot 10^{-5}$ (0)
H ₃ O ⁺	$1 \cdot 10^{-4}$ (0)	$3 \cdot 10^{-4}$ (0)	$1 \cdot 10^{-4}$ (0)	$1 \cdot 10^{-4}$ (0)	$3 \cdot 10^{-4}$ (0)
O ₂ H ⁺	$4 \cdot 10^{-5}$ (0)	$1 \cdot 10^{-4}$ (0)	$5 \cdot 10^{-5}$ (0)	$4 \cdot 10^{-5}$ (0)	$1 \cdot 10^{-4}$ (0)
SO ⁺	$4 \cdot 10^{-5}$ (0)	$7 \cdot 10^{-5}$ (0)	$3 \cdot 10^{-5}$ (0)	$6 \cdot 10^{-5}$ (0)	$8 \cdot 10^{-5}$ (0)
HS ⁺	$2 \cdot 10^{-6}$ (0)	$3 \cdot 10^{-6}$ (0)	$2 \cdot 10^{-6}$ (0)	$3 \cdot 10^{-6}$ (0)	$4 \cdot 10^{-6}$ (0)
N _{e-}	75 (70)	78 (70)	40 (36)	145 (137)	156 (140)
N _{ion}	45 (40)	48 (40)	24 (20)	87 (80)	95 (80)
Europa's source strength, ions/s	2×10^{27} (0)	3.4×10^{27} (0)	1.7×10^{27} (0)	3×10^{27} (0)	3×10^{27} (0)

Densities are in cm^{-3} . Case a, normal parameters characteristic of Europa's environment. Case b, enlarged energetic particle flux. Case c, reduced iogenic corotating flux. Case d, enlarged iogenic corotating flux. Case e, reduced transport rate. The number densities for the case of no Europa are given in parentheses.

presenting the measured quantity versus the incident energy of the electrons or ions, as in *Kieffer* [1969], and if two or more different sets of Arrhenius' coefficients were given, we chose the most recent of them. *Millar et al.* [1991] summarized rate coefficients of 2880 gas-phase reactions among 313 species involving 12 elements for use in astrochemical models; part of this data was used in our model.

Equations (1) were solved numerically by starting with an empty magnetosphere, turning on the sources and sinks and integrating the equations over time until (after some 50-100 days) the number density of all the species reached steady state. For comparison, we run the model with no Europa source to determine what the plasma conditions would be without Europa.

RESULTS AND DISCUSSION

The steady state densities calculated for various transport rates, iogenic corotating flux and energetic particle flux are shown in Table 6. In order to study the sensitivity of the model to the input parameters, five different sets of input parameters were used. Parameters characteristic of Europa's environment are presented as case *a*. In case *b* the energetic particle flux was enlarged by a factor of 2. The iogenic corotating flux was multiplied and divided by 2 in cases *c* and *d*, respectively. The influence of the transport rate was examined by reducing it by half in case *e*. For each set of results the number densities which result if there were no Europa source are given in parentheses.

Pickup oxygen ions at $9.4 R_J$ would fill a shell in phase space at ≈ 874 eV and would not be resolved in the PLS spectra. Spectra not near the magnetic equator have low count rates with no distinct current peaks indicative of a tenuous, hot plasma. During equator crossings, additional well resolved Maxwellian spectra are observed, as shown in the spectra in Figures 2*a* and 2*b*. The common cold temperature of these ions and the presence of high-ionization states and alkali ions are consistent with transport from the Io's orbit over a timescale long enough for thermalization to occur. (We note that the question of whether plasma transport from Io outward is adiabatic or whether heating occurs remains an outstanding issue [*Abe and Nishida*, 1986].) The need, dictated by the shape of the spectrum, to place an ion between those of mass-to-charge ratios of 16 and 23 raises the question whether it is a local water group ion, H_2O^+ or OH^+ or another ion such as doubly ionized potassium. The resolution of the PLS instrument along with the possibility of nonzero spacecraft potential, does not allow us to differentiate uniquely between adjacent values of mass-to-charge ratios such as 17, 18, and $19\frac{1}{2}$ which might be ascribed to OH^+ , H_2O^+ , and K^{++} respectively. We refer the reader to the companion paper by *McNutt* [this issue] for the physical considerations of why this peak should be associated with doubly ionized potassium.

Our calculated values of the parameters which are characteristic of Europa's environment are presented as case *a* of Table 6 and as shown in Figure 4. An interesting result of the model comes from the comparison between the number densities of the ions with and without Europa. A neutral cloud of water fragments with a density greater than 20 molecules per cm^3 , none of which would exist without the sputtering process, is immersed in the torus plasma. With or without Europa source, the density of sulfur and alkali met-

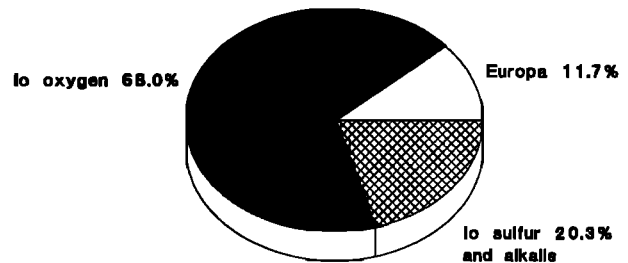


Fig. 4. Calculated composition distribution at Europa's orbit for case *a*.

al ions is the same; a Europa source causes the total density to increase from ~ 40 to ~ 50 cm^{-3} due to the enhancement of the water group ion plasma from Europa. Thus the contribution of Europa, while insignificant in comparison with the Io torus source, nonetheless affects the plasma composition locally. This is consistent with the results of *Bagenal et al.* [1992], which show that oxygen to sulfur ratio increases outside the hot torus, consistent with a Europa source.

During the parameter study the following results were found:

1. Photo-sputtering is an insignificant process. It contributes at most one half of one percent to the number density of certain species such as OH and OH^+ .
2. Elimination of the atomic processes occurring in the Europa torus increases the neutral cloud of water fragments by two orders of magnitude, leaving the ion densities and partitioning almost unchanged.
3. A change in the energetic particle flux causes only a slight change in the water-group neutral and ion number densities. It does however affect Europa's source strength since the sputtering rate is also changed. This is due to the overwhelming effect of the transport.
4. Changing the Io's source strength by a factor of two leads to almost similar changes in the number densities and to a smaller effect in Europa's source strength.
5. An increase (decrease) in the transport rate is almost equivalent to a decrease (increase) in the Io's source strength.

Seveka and Johnson [1982] computed the Europa source rate to be $8 \times 10^{26} s^{-1}$, as was previously estimated by *Johnson et al.* [1981]. Our model, which includes sputtering caused by both corotating iogenic thermal plasma ions and radiation belt particles, gives a source strength ~ 2.5 times greater. The sputtering yields used here for perpendicular incidence to the surface [*Johnson et al.*, 1989]. The yields (and thus the source strength) are enhanced for nonnormal incidence.

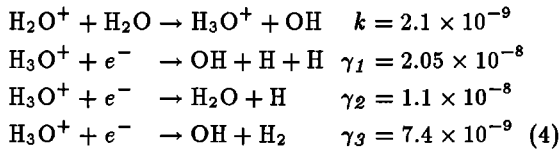
Particles originating at Europa diffuse inward as well as outward, and it is of interest to ask if they can make a significant contribution to the resolution of the Io energy crisis discussed by *Shemansky* [1988] and by *Smith et al.* [1988]. If the pickup energy is 1 keV and the source strength is as given in Table 6, the power added to the Io torus, including adiabatic heating, would be $\sim 3 \times 10^{12}$ W if all particles reaches the torus. In fact, only 10% of them will diffuse inward, so Europa will not greatly affect the energy balance of the Io torus.

The degree of ionization in the plasma can be obtained by dividing the total ion number density by the total charge (electron) density. Typical values for the warm and cold

Io tori are $\sim 4/3$. The degree of ionization increases to $\sim 5/3$ in the outer regions of the warm torus, which may be understood in light of the local enhancement of suprathermal electron flux in this region as reported by *McNutt et al.* [1990].

As might be expected, the results are sensitive to the transport rate and plasma temperature. Early estimates [*Eviatar et al.*, 1985] predicted that there would be no Europa torus because the ions would be swept away in the rapid outwash of the Io matter. Reducing the transport rate from $4 \times 10^{-4} R_J^2 \text{ s}^{-1}$ to $2 \times 10^{-4} R_J^2 \text{ s}^{-1}$ (case *e*), increases the total number density to $\sim 100 \text{ cm}^{-3}$, which contradicts observations. A higher transport rate ($8 \times 10^{-4} R_J^2 \text{ s}^{-1}$) reduces the total number density (which includes the iogenic ions) to $\sim 20 \text{ cm}^{-3}$, much less than the observed values. Since the source strength and diffusion rate are both observationally constrained (determined by Io torus) the calculated densities appear quite reasonable.

One might ask why the ratio of H_3O^+ to H_2O^+ is as low as 5×10^{-4} , whereas in a cometary coma H_3O^+ is the most abundant ion within 20,000 km of the nucleus [*Balsiger*, 1990]. The main reactions with which H_3O^+ is involved and their rate coefficients (in units of $\text{cm}^3 \text{ s}^{-1}$) are



For a Europa collision frequency of $c = 2.4 \times 10^{-8} \text{ s}^{-1}$ and a transport rate of $\frac{1}{\tau} = 1 \times 10^{-5} \text{ s}^{-1}$ the rate equation

$$\begin{aligned} \frac{dn_{\text{H}_3\text{O}^+}}{dt} &= k \times n_{\text{H}_2\text{O}} \times n_{\text{H}_2\text{O}^+} \\ &- \left[\frac{1}{\tau} + c + (\gamma_1 + \gamma_2 + \gamma_3) \times n_e \right] \times n_{\text{H}_3\text{O}^+} \end{aligned} \quad (5)$$

gives for steady state the ratio:

$$\frac{n_{\text{H}_3\text{O}^+}}{n_{\text{H}_2\text{O}^+}} = \frac{k \times n_{\text{H}_2\text{O}}}{(\gamma_1 + \gamma_2 + \gamma_3) \times n_e + \left(\frac{1}{\tau} + c\right)} \approx 2 \times 10^{-4} \quad (6)$$

where the electron and the neutral water densities are 75 and 1.3 cm^{-3} , respectively, according to the results of case *a*. Despite the neglect of atomic interaction with the other ions and neutral species, this value is close to the model ratio, which indicates that reactions (4) are the most significant processes in the plasma. This insignificance of H_3O^+ (in contrast to cometary comea) is a result of the large dissociative recombination rate and the low abundance of neutral water molecules.

CONCLUSIONS

Matter sputtered off the surface of Europa differs in composition and energy spectrum from Io torus matter. If ionized by electron impact ionization near Europa, molecular ions will have very broad energy spectra and thus should be distinguishable from the cold matter that has diffused out from the Io torus. Both PLS spectra and the model results show a partitioning of ~ 40 (cold) ions per cm^3 of Io origin and 5-10 (warm) ions per cm^3 , presumably of Europa origin.

We have shown that a Europa source results in an enhancement of the total abundance of oxygen-bearing con-

stituents. If we bear in mind that the creation of most O^{++} takes place in the outer reaches of the Io torus, where suprathermal electrons were observed [*McNutt et al.* 1990], we can explain the nonsimilarity in the sulfur and oxygen abundance reported by *Bagenal et al.* [1992].

If we ignore Europa's contribution to the plasma environment we are led to a picture contrary to observation. We must therefore conclude that Europa's surface is sputtered by iogenic matter and is, therefore, a source of magnetospheric plasma. If there were no effective Europa source, no intensification would have been observed in the abundance of oxygen ions and their profile would resemble that of iogenic sulfur. The survival of eurogenic water group ions will depend on the transport rate. We have shown that the transport rate at Europa orbit must satisfy $5 \times 10^{-6} \leq 1/\tau \leq 2 \times 10^{-5} \text{ s}^{-1}$ in order that densities comparable to those observed be derived by the model. This rate is not consistent with L^3 diffusion and the observed transport rate at Io. *Siscoe et al.* [1981] point out that the strong gradient in flux tube content on the outside ledge of the warm torus implies the diffusion exponent is as large as 12. *Thorne* [1983] shows that this value of the exponent fits the *Armstrong et al.* [1981] observations of the intermediate energy particles (magnetic moment of 70 MeV/G) very well. Although Europa's contribution to the total plasma content is small compared to that of the Io torus, it has an effect on the local plasma composition. From the model, we estimate Europa's source strength as 2×10^{27} molecules per second (case *a*).

Huang and Siscoe [1987] have classified Europa's torus as heterogenic and heterotropic, that is, generated by sputtering from an external source with a transport mechanism externally imposed. We have demonstrated that the strong diffusion induced by the iogenic plasma inhibits the growth of the Europa torus and prevents it from reaching densities comparable to those of the Io torus. In the absence of a strong Io source, the transport rate would be lower, and would result in a denser and larger Europa torus. Transport might then become autotropic, that is, self-driven and self-limiting.

Had the SWICS instrument of Ulysses [*Geiss et al.*, 1992] been operative at the equatorial plane, it might have differentiated iogenic potassium ions from lighter European water group ions. Since the scale height of pickup water ions is much larger than that of cold iogenic potassium ($6.7 R_J$ compared to $0.33 R_J$), any intermediate A/Z ions detected by Ulysses far from the plane will be associated with the presence of the Europa plasma source. Indeed, a tentative identification of water group ions is made by *Geiss et al.* [1992] on the basis of preliminary Ulysses data analysis. Further analysis of data from Ulysses and from the forthcoming Galileo encounter is expected to provide an ultimate resolution of this question. We expect the Galileo spacecraft to find, either by means of observation of UV emission or by using a mass spectrometer, a neutral cloud of hydrogen, oxygen, and water molecules at the orbit of Europa. The plasma instrument will measure a small increase of $\sim 10\%$ in the local number density (attributed mostly to water group ions) and a small reduction in the ionization state at that location. A residual Europa atmosphere is a most speculative idea but certainly worth examining (by occultation techniques).

APPENDIX: RELATION OF TRANSPORT AND SOURCE TERMS TO THE DIFFUSION COEFFICIENT

Equations (1) in the text are formulated in terms of the total content N of the various species within the volume V of the Europa torus. Plasma flow into and out of the volume is represented by the diffusion term

$$\frac{1}{r} \frac{\partial}{\partial r} \left[r B D \frac{\partial}{\partial r} \left(\frac{nh}{B} \right) \right] \quad (\text{A1})$$

where D is the diffusion coefficient assumed, for simplicity, to vary as a power law in the radial distance r ,

$$D = D_E \left(\frac{r}{r_E} \right)^\nu \quad (\text{A2})$$

where D_E and r_E are the values at the orbit of Europa, n is the equatorial number density (related to N of equation (1) by $n = N/V$), h is the scale height of the torus along the magnetic field and $B \propto r^{-3}$ is the equatorial magnetic field strength. We wish to approximate the term (A1) by the simple forms of equation (1), I for plasma input from the Io torus and $-N/\tau$ for plasma loss.

Evaluation of τ

We consider first only the contribution of plasma from within the volume of the Europa torus, $r_E - \Delta r < r < r_E + \Delta r$. We define $x \equiv r - r_E$ and write (in the steady state limit)

$$D_E \frac{\partial^2 n}{\partial x^2} + Q = 0 \quad -\Delta r < x < \Delta r \quad (\text{A3})$$

where Q represents all the local nontransport source and loss terms of equation (1) and $\Delta r \ll r_E$ has been used to neglect all variation of D , r , B and h in (A1). Equation (A3) has the solution

$$n = -\frac{1}{2} \frac{Q}{D_E} x^2 + C_1 x + C_2 \quad (\text{A4})$$

where C_1 and C_2 are integration constants. The total diffusive flux at a given distance r is given by

$$S = -2\pi r B D \frac{\partial}{\partial r} \left(\frac{nh}{B} \right) \quad (\text{A5})$$

and the difference between the values of S at $r = r + \Delta r$ (outward of the source, S_{out}) and $r = r_E - \Delta r$ (inward, S_{in}) determines C_1 ; from (A4) we obtain the following relations:

$$\begin{aligned} S_{\text{out}} &= 2\pi r_E Q \Delta r - C^* \\ S_{\text{in}} &= -2\pi r_E Q \Delta r - C^* \end{aligned} \quad (\text{A6})$$

where $C^* = 2\pi r_E D_E C_1$. If we define ϵ as the ratio of inward to total flux,

$$\epsilon = \frac{-S_{\text{in}}}{S_{\text{out}} - S_{\text{in}}},$$

then equation (A6) becomes

$$\begin{aligned} S_{\text{out}} &= 2\pi r_E Q \Delta r (2 - \epsilon) \\ S_{\text{in}} &= -\epsilon 2\pi r_E Q \Delta r \end{aligned} \quad (\text{A7})$$

The loss time τ is evidently defined by

$$\begin{aligned} Q\tau &= \bar{n} \\ Q\tau &= C_2 - \frac{1}{6} \frac{Q}{D_E} (\Delta r)^2 \end{aligned} \quad (\text{A8})$$

where \bar{n} is the value of n averaged over the interval $-\Delta r < x < \Delta r$. The value of C_2 is fixed by matching (A4) to solutions of the diffusion equation in the external region $r > r_E + \Delta r$. Since there are no sources in this region, S , which is given by (A5) is constant and must be equal to S_{out} which is given by (A7). For D given by (A2) the solution for n in the region $r > r_E$ is:

$$\begin{aligned} n(r) &= \frac{S_{\text{out}}}{2\pi D_E h} \int_{r_E}^R dx x^{\nu-2} \\ n(r) &= \frac{S_{\text{out}}}{2\pi D_E h} \log \left(\frac{R}{r} \right) \quad \nu = 3 \\ n(r) &= \frac{S_{\text{out}}}{2\pi D_E h} \frac{1}{\nu-3} \left[\left(\frac{r_E}{r} \right)^{\nu-3} - \left(\frac{r_E}{R} \right)^{\nu-3} \right] \quad \nu \neq 3 \end{aligned} \quad (\text{A9})$$

where R is the distance at which $n = 0$. Equating $n(r_E)$ to \bar{n} gives C_2 ; to lowest order in $\frac{\Delta r}{r}$, the result is

$$\frac{1}{\tau} = \frac{D_E}{2r_E \Delta r} \xi, \quad (\text{A10})$$

where

$$\begin{aligned} \frac{1}{\xi} &= (1 - \epsilon) \log \left(\frac{R}{r_E} \right) \quad \nu = 3 \\ \frac{1}{\xi} &= \frac{1 - \epsilon}{\nu - 3} \left(1 - \frac{r_E}{R} \right)^{\nu-3} \quad \nu \neq 3 \end{aligned} \quad (\text{A11})$$

and the factor ξ may be regarded as of order unity. The value of ϵ must be assumed to be very small; the flux S_{in} of Europa-generated plasma is also constant for $r < r_E$ and hence equal to its value at $r = 6 R_J$, but for $r < 6 R_J$ diffusion is generally assumed to be extremely weak.

Evaluation of I

We now consider only the contribution of plasma coming from the Io torus. With all the Europa-related and non-transport terms neglected, equation (1) in the steady state limit can be reduced to:

$$\frac{I}{V} = \frac{n}{\tau} \quad (\text{A12})$$

where n is to be taken as the density at $r = r_E$ produced by diffusion from an Io source of strength S and τ is defined by (A8). The value of n is now given by a solution identical to (A9) except for the replacement of S_{out} by S :

$$n(r_E) = \frac{S}{2\pi D_E h} \int_1^{\frac{R}{r_E}} dx x^{\nu-2} \quad (\text{A13})$$

Combining (A13) with (A8) and recognizing that the same integral occurs in both, we obtain

$$\frac{I}{V} = \frac{S}{4\pi r_E h \Delta r (1 - \epsilon)} \quad (\text{A14})$$

For reasons already stated, ϵ may be neglected.

Acknowledgments. The work at Tel Aviv University was supported in part during the initial stages by the United States-Israel Binational Science Foundation under grant 88-00120 and in the latter stages by the German-Israeli Foundation for Scientific Research and Development under grant I-0199-163.07/91. The work at the Max-Planck Institut für Aeronomie was supported in part by the German-Israeli Foundation for Scientific Research and Development under the same grant. The MIT portion of this work was supported by NASA under contract 959203 from the Jet Propulsion Laboratory to the Massachusetts Institute of Technology and by NASA grant NAGW 1622. The work at UCLA was supported by the National Aeronautics and Space Administration under grant NAGW-87. Aharon Eviatar expresses his apprecia-

tion for the hospitality of the Department of Atmospheric Sciences of UCLA during the summer of 1992. Ron Schreier acknowledges helpful discussions with Amiel Sternberg. We are grateful to T. J. Millar for allowing us to use the UMIST ratfile and to Ralph L. McNutt, Jr. for helpful suggestions.

The Editor thanks two referees for their assistance in evaluating this paper.

REFERENCES

- Abe, T., and A. Nishida, Anomalous outward diffusion and associated heating of ionogenic ions in the Jovian magnetosphere, *J. Geophys. Res.*, **91**, 10,003–10,011, 1986.
- Armstrong, T.P., M.T. Paonessa, S.T. Brandon, S.M. Krimigis, and L.J. Lanzerotti, Low energy charged particle observations in the 5–20 R_J region of the Jovian magnetosphere, *J. Geophys. Res.*, **86**, 8342–8355, 1981.
- Bagenal, F., Plasma conditions inside Io's orbit, *J. Geophys. Res.*, **90**, 311–324, 1985.
- Bagenal, F., Torus-magnetosphere coupling, in *Time-Variable Phenomena in the Jovian System*, edited by M.J.S. Belton, R.A. West, and J. Robe, *NASA Spec. Publ.*, SP-494, 196–210, 1989.
- Bagenal, F., D.E. Shemansky, R.L. McNutt Jr., R. Schreier, and A. Eviatar, The abundance of O^{++} in the Jovian magnetosphere, *Geophys. Res. Lett.*, **19**, 79–82, 1992.
- Balsiger, H., Measurements of ion species within the coma of comet Halley from Giotto, in *Comet Halley*, vol. 1., edited by J. Mason, pp. 129–146, Ellis Horwood Limited, England, 1990.
- Banks, P.M., and G. Kockarts, in *Aeronomy, Part A*, Academic, San Diego, Calif., 1973.
- Bar-Nun, A., G. Herman, M.L. Rappaport, and Yu. Mekler, Ejection of H_2O , O_2 , H_2 and H from water ice by 0.5–6 keV H^+ and Ne^+ ion bombardment, *Surface Sci.*, **150**, 143–156, 1985.
- Belcher, J.W., The low-energy plasma in the Jovian magnetosphere, in *Physics of the Jovian Magnetosphere*, edited by A.J. Dessler, pp. 68–105, Cambridge University Press, New York, 1983.
- Bond, J. B. Jr., K. M. Watson, and J. A. Welch Jr., *Atomic Theory of Gas Dynamics*, Addison-Wesley, New York, Reading, Mass., 1966.
- Bridge, H.S., J.W. Belcher, R.J. Butler, A.J. Lazarus, A.M. Mavretic, J.D. Sullivan, G.L. Siscoe and V.M. Vasyliunas, The plasma experiment on the 1977 Voyager mission, *Space Sci. Rev.*, **21**, 259–287, 1977.
- Brown, R.A., C.B. Pilcher, and D.F. Strobel, Spectrophotometric studies of the Io torus, in *Physics of the Jovian Magnetosphere*, edited by A.J. Dessler, pp. 197–225, Cambridge University Press, New York, 1983.
- Brown, R.A., D.E. Shemansky, and R.E. Johnson, A deficiency of OIII in the Io plasma torus, *Astrophys. J.*, **264**, 309–323, 1983.
- Eviatar, A., C.F. Kennel, and M. Neugebauer, Possible origins of time variability in Jupiter's magnetosphere, III, Variations in the heavy ion plasma, *Geophys. Res. Lett.*, **5**, 287–290, 1978.
- Eviatar, A., G.L. Siscoe, T.V. Johnson, and D.L. Matson, Effects of Io ejecta on Europa, *Icarus*, **47**, 75–83, 1981.
- Eviatar, A., A. Bar-Nun, and M. Podolak, European surface phenomena, *Icarus*, **61**, 185–191, 1985.
- Fehsenfeld, F.C., A.L. Schmeltekopf, and E.E. Ferguson, Thermal-energy ion-neutral reaction rates, VII, Some hydrogen-atom abstraction reactions, *J. Chem. Phys.*, **46**, 2802–2808, 1967.
- Geiss, J., et al., Plasma composition in Jupiter's magnetosphere: Initial results from the Solar Wind Ion Composition Spectrometer, *Science*, **257**, 1535–1539, 1992.
- Harrison, H., and R.I. Schoen, Evaporation of ice in space: Saturn's rings, *Science*, **157**, 1175–1176, 1967.
- Huang, T.S., and G.L. Siscoe, Types of planetary tori, *Icarus*, **70**, 366–378, 1987.
- Intriligator, D.S., and W.D. Miller, First evidence for a Europa plasma torus, *J. Geophys. Res.*, **87**, 8081–8090, 1982.
- Johnson, R.E., L.J. Lanzerotti, W.L. Brown, and T.P. Armstrong, Erosion of Galilean satellite surfaces by Jovian magnetosphere particles, *Science*, **212**, 1027–1030, 1981.
- Johnson, R.E., M.K. Pospieszalska, E.C. Sittler, Jr. A.F. Cheng, L.J. Lanzerotti, and E.M. Sieveka, The neutral cloud and heavy ion inner torus at Saturn, *Icarus*, **77**, 311–329, 1989.
- Kieffer, L.J., Low-energy electron-collision cross-section data, I, Ionization, dissociation, vibrational excitation, *At. Data*, **1**, 19–89, 1969.
- Lotz, W., Electron impact ionization cross sections and ionization rate coefficients for atoms and ions, *Astrophys. J. Suppl. Ser.*, **14**, 207–238, 1967.
- Massey, H.S.W., and H.B. Gilbody, Electronic and ionic impact phenomena, in *Recombination and Fast Collisions of Heavy Particles*, vol. IV, p. 2782, Oxford University Press, New York, 1974.
- McNutt, R.L., Possible in situ detection of K^{2+} in the Jovian magnetosphere, *Eos Trans. AGU*, **63**, 1062, 1982.
- McNutt, R.L., J.W. Belcher, and H.S. Bridge, Positive ion observations in the middle magnetosphere of Jupiter, *J. Geophys. Res.*, **86**, 8319–8342, 1981.
- McNutt, R.L. Jr., F. Bagenal, and R.M. Thorne, Observations of auroral secondary electrons in the Jovian magnetosphere, *Geophys. Res. Lett.*, **17**, 291–294, 1990.
- McNutt, R.L., Possible in situ detection of K^{2+} in the Jovian magnetosphere, *J. Geophys. Res.*, this issue.
- Millar, T.J., J.M.C. Rawlings, A. Bennett, P.D. Brown, and S.B. Charney, Gas phase reactions and rate coefficients for use in astrochemistry. The UMIST ratfile. *Astron. Astrophys. Suppl. Ser.*, **87**, 585–619, 1991.
- Mul, P.M.J., J.W. McGowan, P. DeFrance, and J.B.A. Mitchell, Merged electron-ion beam experiments, V, Dissociative recombination of OH^+ , H_2O^+ , H_2O^+ , and D_2O^+ , *J. Phys. B.*, **16**, 3099–3107, 1983.
- Richardson, J.D., A. Eviatar, and G.L. Siscoe, Satellite tori at Saturn, *J. Geophys. Res.*, **91**, 8749–8755, 1986.
- Richardson, J.D., and R. L. McNutt Jr., Observational constraints on interchange models at Jupiter, *Geophys. Res. Lett.*, **14**, 64–67, 1987.
- Schmidt, H.U., R. Wegmann, W.F. Huebner, and D.C. Boice, Cometary gas and plasma flow with detailed chemistry, *Comp. Phys. Commun.*, **49**, 17–59, 1988.
- Shemansky, D.E., Energy branching in the Io plasma torus: The failure of neutral cloud theory, *J. Geophys. Res.*, **93**, 1773–1784, 1988.
- Sieveka, E.M., and R.E. Johnson, Thermal and plasma-induced molecular redistribution on the icy satellites, *Icarus*, **51**, 528–548, 1982.
- Siscoe, G.L., and C.-K. Chen, Io: A source for Jupiter's inner plasmasphere, *Icarus*, **31**, 1–10, 1977.
- Siscoe, G.L., A. Eviatar, R.M. Thorne, and J.D. Richardson, Ring current impoundment of the Io plasma torus, *J. Geophys. Res.*, **86**, 8480–8484, 1981.
- Sittler, E.C., Jr., and D.F. Strobel, Io plasma torus electrons, *J. Geophys. Res.*, **92**, 5741–5762, 1987.
- Smith, R.A., F. Bagenal, A.F. Cheng, and D.F. Strobel, On the energy crisis in the Io plasma torus, *Geophys. Res. Lett.*, **15**, 545–548, 1988.
- Squyres, S.W., R.T. Reynolds, P.M. Cassen, and S.J. Peale, Liquid water and active resurfacing on Europa, *Nature*, **301**, 225–226, 1983.
- Stebbing, R.F., A.C.H. Smith, and H. Ehrhardt, Charge transfer between oxygen atoms and O^+ and H^+ ions, *J. Geophys. Res.*, **69**, 2349–2355, 1964.
- Thorne, R.M., Microscopic plasma processes in the Jovian magnetosphere, in *Physics of the Jovian Magnetosphere*, edited by A.J. Dessler, pp. 454–488, Cambridge University Press, New York, 1983.
- A. Eviatar and R. Schreier, Department of Geophysics and Planetary Science, The Raymond and Beverly Sackler Faculty of Exact Sciences, Tel Aviv University, 69978 Ramat Aviv, Israel.
- J. D. Richardson, Center for Space Research, Massachusetts Institute of Technology, Cambridge MA 02139.
- V. M. Vasyliunas, Max-Planck-Institut für Aeronomie, D-3411, Katlenburg-Lindau, Germany.

(Received February 16, 1993;
revised June 14, 1993;
accepted July 22, 1993.)